Observation of wall stabilization and active control of low-*n* magnetohydrodynamic instabilities in a tokamak*

T. H. Ivers,† E. Eisner, A. Garofalo, R. Kombargi, M. E. Mauel, D. Maurer, D. Nadle, G. A. Navratil, M. K. V. Sankar, M. Su, E. Taylor, and Q. Xiao
Department of Applied Physics, Columbia University, New York, New York 10027

R. R. Bartsch, W. A. Reass, and G. A. Wurden
Los Alamos National Laboratory, Los Alamos, New Mexico 87545

(Received 10 November 1995; accepted 2 February 1996)

The High Beta Tokamak-Extended Pulse (HBT-EP) experiment [J. Fusion Energy **12**, 303 (1993)] combines an internal, movable conducting wall with a high-power, modular saddle coil system to provide passive and active control of long wavelength magnetohydrodynamic (MHD) instabilities. Systematic adjustment of the radial position, b, of the conducting wall elements in relation to the surface of the plasma (minor radius a) resulted in the suppression of β-limiting disruptions for discharges in which $b/a<1.2$ and a positive plasma current ramp was maintained. Conducting wall stabilization of kink instabilities was observed in discharges with strong current ramps and in plasmas with β values near the Troyon stability boundary. The frequency of slowly growing modes that persisted in wall-stabilized discharges was controlled by applying oscillating $m=2$, $n=1$ resonant magnetic perturbations. A compact, single-phase saddle coil system permitted modulation of the rotation velocity of internal $m/n=2/1$ instabilities by a factor of 2. © *1996 American Institute of Physics.* [S1070-664X(96)94005-5]

I. INTRODUCTION

A critical objective in the design of an economically attractive, steady-state tokamak fusion reactor is the simultaneous maximization of the plasma pressure, p (parametrized by $\beta \equiv 2\mu_0 p/B_\phi^2$, where B_ϕ is the toroidal magnetic field), the noninductive ''bootstrap'' current, $I_{\rm bs}$, and the energy confinement time, τ_E. Reactor designs based upon this prescription, such as ARIES-II and ARIES-IV,[1] rely on a close-fitting conducting wall surrounding the plasma for stabilization of the $n=1$ external kink mode. A practical wall for kink stabilization is likely to be incomplete (with gaps for flux penetration, auxiliary heating, and diagnostic access) and will possess finite resistivity. These deviations from a symmetric, ideal wall have theoretical implications[2,3] for plasma stability: gaps may reduce the effective conductivity or modify the effective position of the wall; external kinks, under certain conditions, may ''explode'' through the gaps with ideal magnetohydrodynamic (MHD) growth rates; finite resistivity of the wall may destabilize the ''resistive wall mode,'' a kink instability that grows on a time scale characteristic of flux diffusion through the wall.

Operationally, the onset of β-limiting instabilities has been observed in many tokamaks[4] to follow the simple Troyon[5] scaling, $\beta_{\rm max} \propto I_p/aB_\phi$, with a proportionality constant that depends on the details of the current and pressure profiles as well as the shape of the plasma cross section. This stability boundary is generally expressed through the value of the normalized beta, $\beta_N \equiv \beta(\%)/[I_p({\rm MA})/a({\rm m})B_{\phi 0}({\rm T})]$. In the DIII-D tokamak,[6] wall stabilization due to the interaction between the rotating plasma and the vacuum chamber is considered responsible for sustained operation at β values 30% above the Troyon boundary.[7] The installation of a fixed conducting wall resulted in improved performance in the modified Princeton Beta Experiment[8] (PBX-M) over that obtained in the predecessor device, PBX,[9] although direct assessment of the role of the conducting wall was complicated by the requirement that changes in the plasma cross section were necessary to vary the plasma–wall separation. Internal instabilities that persisted in the presence of the conducting wall were implicated in the termination of DIII-D and PBX-M discharges by directly causing disruptions or contributing to arrested plasma rotation. In principle, a reduction in the plasma rotational velocity due to the torque exchanged between wall eddy currents and the plasma not only exacerbates the growth of tearing modes,[10,11] but may lead to ''locked'' modes which have been associated with confinement degradation and disruptions.[12] These considerations suggest that a means of active plasma rotation control and resistive instability suppression must augment a passive conducting wall to ensure reliable, nondisruptive tokamak operation at high values of β.

The High Beta Tokamak-Extended Pulse (HBT-EP) experiment[13,14] was designed to investigate the feasibility of a stable, high-β tokamak using the combination of a close-fitting conducting wall, active mode control, and plasma rotation. The HBT-EP approach emphasizes modular components: the passive stabilizer is a movable conducting wall with 20 independently adjustable segments; active mode suppression and plasma rotation control are accomplished using five pairs of compact, toroidally distributed saddle coils.

The remainder of this paper is organized as follows. Section II is a description of the tokamak as well as the passive and active stabilization systems. Results from wall-stabilization experiments and experiments involving active control of residual instabilities in wall-stabilized discharges

*Paper 5IAl, Bull. Am. Phys. Soc. **40**, 1746 (1995).
†Invited speaker.

 1070-664X/96/3(5)/1926/9/$10.00

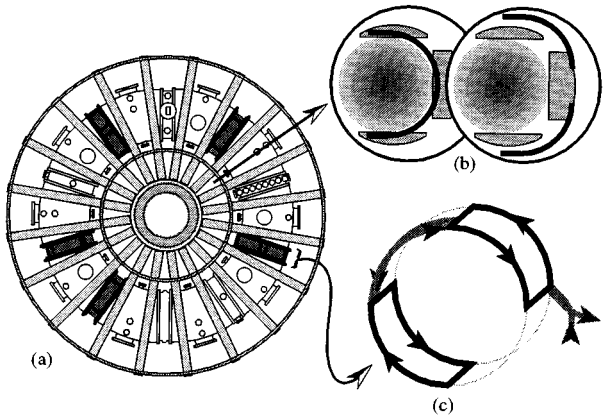

FIG. 1. (a) Top view of the HBT-EP tokamak. (b) Cross section of the vacuum chamber showing poloidal limiters and conducting shells in the inserted and retracted positions. (c) Schematic diagram of one saddle coil pair.

are presented in Sec. III. Finally, a discussion and summary are given in Sec. IV.

II. THE HBT-EP TOKAMAK

HBT-EP (major radius, $R_0=0.92$ m, minor radius, $a=0.15$ m, plasma current, $I_p \leqslant 25$ kA, toroidal field, $B_\phi \approx 3.5$ kG) utilizes rapid plasma formation to attain β values near the Troyon stability boundary. Typical plasma parameters are electron density, $n_{e0} \sim 1\times 10^{19}$ m^3, electron temperature, $T_{e0} \sim 100$ eV, and Lundquist number, $S \sim 10^5$. Figure 1(a) displays a plan view of the tokamak. The vacuum chamber was constructed from ten large stainless steel sections linked at five locations by stainless steel bellows and ''spool'' segments housing the poloidal limiters and diagnostic ports. The remaining chamber segments are linked by quartz cylinders which permit rapid penetration of the Ohmic heating flux and equilibrium fields. In addition, the quartz segments serve as locations for Fourier-analyzing Rogowski coils, Mirnov loops, and high-power saddle coils.

A. Segmented, adjustable conducting wall

A unique feature of the HBT-EP tokamak is an internal, adjustable conducting wall. Each of the ten large vacuum chamber segments contains two wall sections, or ''shells'' [Fig. 1(b)]. The shells were cut from 0.013 m thick spun aluminum and were nickel plated to reduce sputtering. Each of the 20 shells is mounted on an independent, movable support permitting the wall segments to be retracted on a $\pm 45°$ angle to the midplane of the torus. The plasma radius is fixed by a separate set of poloidal limiters. This arrangement allows the shell position to be varied over a range of 0.01–0.09 m from the surface of the plasma ($1.07 \leqslant b/a \leqslant 1.52$, where b is the radial distance of the shells from the plasma center). In the fully inserted configuration, the shells cover 78% of the outboard half of the plasma (39% of the total plasma surface area). The measured eddy-current decay time due to equilibrium magnetic field penetration is $\tau_{n=0} \approx 8$ ms.

B. Modular saddle coils

Active control of MHD instabilities and induced plasma rotation are accomplished through the application of resonant magnet perturbations imposed by a set of modular saddle coils. The coil array consists of five, nine-turn coil pairs; each pair spans only 6° in toroidal angle and generates a magnetic perturbation of dominant poloidal mode number $m=2$. Figure 1(c) shows a schematic representation of one coil pair. The coils are connected in series and positioned outside each of the five quartz vacuum chamber segments to give the applied field a toroidal mode number $n=1$. The coil set is driven by two 10 MW power amplifiers[15] provided under a collaboration with Los Alamos National Laboratory. The amplifiers are transformer coupled to the saddle coils and are capable of delivering ± 600 A current with a bandwidth of 20 kHz.

III. EXPERIMENTAL RESULTS

A. Wall stabilization of kink modes

The effectiveness of the segmented conducting shells in suppressing kink instabilities was demonstrated using two types of discharges. In the first type, designated ''current-ramp'' discharges, plasmas were formed with a sustained current ramp of $dI_p/dt \sim 6$ MA/s to induce a broad current profile with enhanced edge currents. Ideal MHD theory predicts that plasmas possessing finite current or current gradients at the plasma boundary are susceptible to external kink instabilities in the absence of a conducting wall independent of the value of β.[16,17] These instabilities are predicted to occur below integer values of the edge safety factor, $q(a)$, where $q(a) \equiv (1/2\pi)\int_0^{2\pi} (rB_\phi/RB_\theta)_{r=a} d\theta$ for a circular cross-section plasma.

The role of the shells in preventing β-limiting disruptions was examined in the second type of plasma, designated ''rapid-formation'' discharges. This formation scheme utilized a fast startup ($dI_p/dt \sim 100$ MA/s) followed by a moderate current ramp to produce plasmas that attained values of $\beta_N \approx 2$. With the shells retracted, these plasmas disrupted near $\beta_N \sim 1.5$ following the rapid growth of a global instability. This value of β_N is consistent with the predicted stability boundary to ideal external kinks in the absence of a conducting wall.

1. Current-ramp discharges

Figure 2 compares the time evolution of two current-ramp discharges, one formed with the conducting shells fully inserted ($b/a=1.07$) and the other with the shells fully retracted ($b/a=1.52$). The plasma parameters in both cases were maintained as identical as possible. The toroidal field was held constant, so that the ramping plasma current produced a cylindrical edge safety factor, $q^* \equiv 2\pi a^2 B_{\phi 0}/\mu_0 I_p R_0$, that decreased as a function of time.

In the discharge formed with the shells retracted, magnetic fluctuations appeared at $t=1.7$ ms, at which time $q^* \approx 3.6$. Toroidally distributed, Fourier-analyzing Rogowski coils and Mirnov loops indicated that the structure of the perturbation was predominantly poloidal mode number $m=3$ with toroidal mode number $n=1$. Initially, the instability

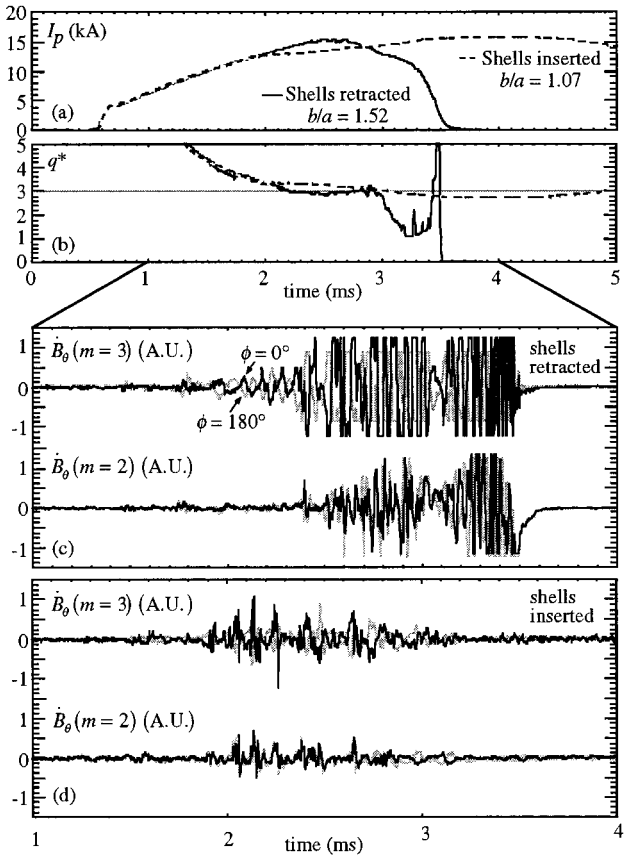

FIG. 2. Comparison of ''current-ramp'' discharges with shells inserted and shells retracted showing (a) plasma current, (b) cylindrical safety factor, (c) $m=3$ and $m=2$ magnetic activity at toroidal locations $\phi=0°$ and $\phi=180°$ with shells retracted, and (d) shells inserted.

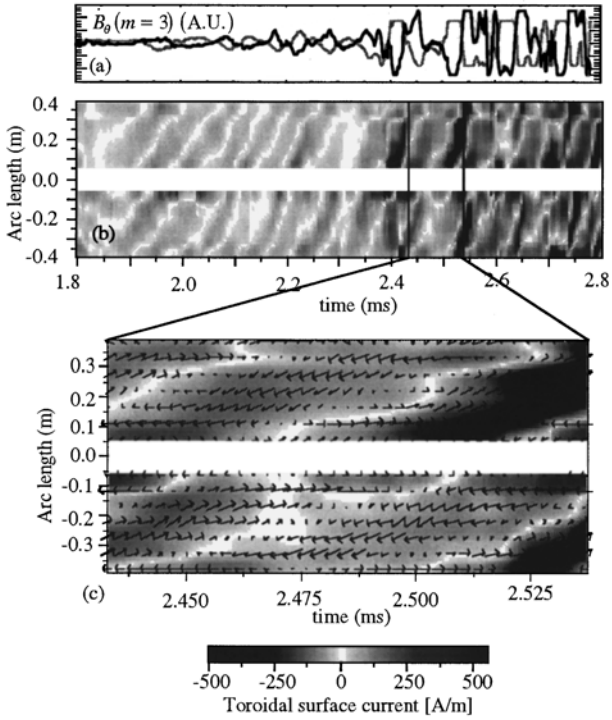

FIG. 3. (a) Disruption precursor $m=3$ magnetic fluctuations at $\phi=0°$ and $\phi=180°$. (b) Measured eddy current pattern on the segmented conducting shells in the retracted position (gap between shells is at outer midplane). (c) Comparison of measured (shaded) and simulated (arrows) shell eddy currents.

grew with a characteristic growth time $\gamma^{-1}\approx 345\ \mu$s, after which the fluctuations maintained an amplitude of $\delta B_\theta/B_\theta(r=a)\approx 0.7\%$ for 500 μs. However, as q^* dropped below 3, the mode amplitude doubled in less than 30 μs. This instability resulted in immediate termination of the current ramp and, after approximately 1 ms, a complete current quench ended the discharge.

The eddy currents induced in the conducting shells by the instability were deduced from magnetic field measurements. The magnetic probes are mounted directly on two shells located above and below the midplane. The boundary condition at the shells may be expressed as $\tilde{\boldsymbol{\kappa}}=\hat{n}\times[\tilde{\mathbf{B}}(\text{out})-\tilde{\mathbf{B}}(\text{in})]/\mu_0$, where $\tilde{\boldsymbol{\kappa}}$ is the fluctuating surface current, $\hat{n}$ is the unit vector normal to the surface of the shells, and $\tilde{\mathbf{B}}$(out) and $\tilde{\mathbf{B}}$(in) refer to the magnetic field on the outer and plasma-facing side of the shells. In this case, the frequency of the disruption precursors ($f_{m=3}\approx 10$ kHz) was sufficiently high that the shells appeared to be perfectly conducting ($f\tau_{\text{wall}(m=3)}\sim 20$), so only the plasma-facing coils were used in the analysis. The time history of the toroidal component of the eddy currents is displayed in Fig. 3(b). Note that the two shells support segments of a helical current pattern, even though the helical currents must close individually on each shell segment. The pitch of the current pattern (a function of both frequency and mode structure) did not change greatly during the evolution of the instability, although the eddy current amplitude was manifestly larger after the time at which $q^*<3$. The measured pattern displays good agreement to the pattern theoretically predicted to result from an $m/n=3/1$ external mode with the conducting shells retracted [Fig. 3(c)]. The arrows represent the simulated eddy currents calculated using the PEST/VACUUM ideal MHD codes[18] modified to include the poloidally segmented shells, and the shaded contours display one period of the linearly interpolated κ_ϕ measurements from 16 shell-mounted probes.

For the plasma formed with the shells fully inserted ($b/a=1.07$), similar magnetic fluctuations appeared at $q^*\approx 3.5$. As in the ''shells-retracted'' case, the instability possessed an $m/n=3/1$ magnetic structure, although these fluctuations were nonsinusoidal (perhaps due to interaction with the shells) and were accompanied by bursts of $m=2$, even-n fluctuations. This internal instability appears to have produced a reduction in the plasma current-ramp rate, possibly due to increased plasma resistivity, during the evolution of q^* from 3.6 to 3. As q^* dropped below 3, however, the fluctuations disappeared and quiescent operation ensued, in marked contrast to the disruptive plasma formed with the shells retracted.

These examples demonstrate the effectiveness of the segmented shells in stabilizing a kink instability as it evolves from a tearing-type perturbation, with the $q=m/n$ resonant surface (in this case 3/1) within the plasma to an external mode in which the resonant surface lies outside the

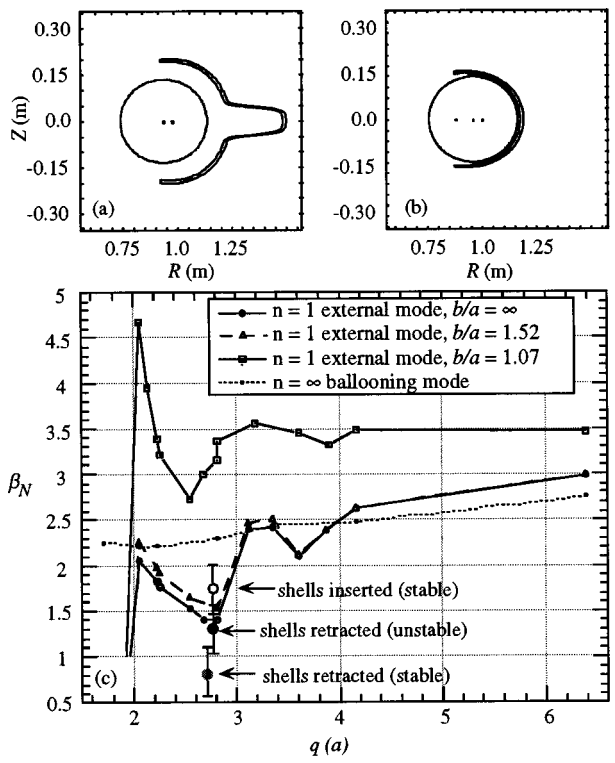

FIG. 4. PEST/VACUUM code model for segmented shells showing (a) retracted and (b) inserted configurations. (c) Calculated ideal stability diagram for HBT-EP plasmas showing measured β_N values for three "rapid-formation" discharges.

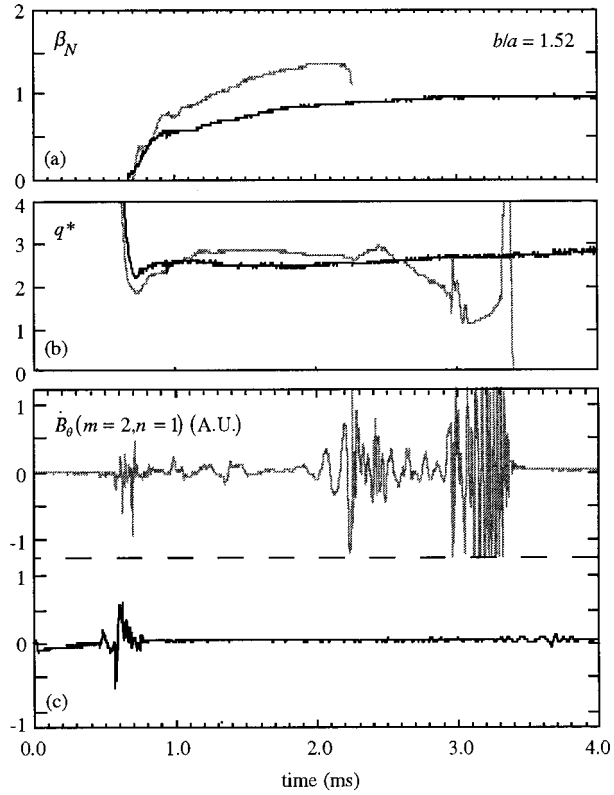

FIG. 5. Comparison of quiescent and disruptive discharges formed with the shells retracted showing time evolution of (a) normalized beta, (b) cylindrical q and (c) $m/n=2/1$ magnetic fluctuations.

plasma. The disruption caused by the external kink was prevented by the close-fitting shells. However, it was also observed that the conducting shells did not completely suppress internal modes. Although the residual instabilities in these discharges did not cause a disruption, they did have a somewhat deleterious effect on the plasma. Experiments demonstrating the control of internal instabilities are described in Sec. III C.

2. Beta-limited discharges

In the previous examples, the 6 MA/s current ramp resulted in relatively weak Ohmic heating and consequently a value of $\beta_N<1$ at the time of disruption for the "shells-retracted" discharge. Rapid formation of the plasma ($dI_p/dt\sim100$ MA/s) produces sustained $q^*\leqslant3$ plasmas with β values that exceed the ideal external kink stability limit. Figure 4(c) shows the ideal MHD stability boundaries for HBT-EP discharges calculated using the PEST-II[19] code. Conventional (monotonic) profiles with no edge currents were used in the free-boundary equilibria from which the stability limits were determined. Although a direct measurement of the plasma current profile was not available, equilibria reconstructed using magnetic measurements of the poloidal field in the shadow of the limiter were consistent with small edge currents in "rapid formation" discharges at $t>1.5$ ms after formation. The pressure profiles ($p_0/\langle p\rangle\approx3$) used were consistent with those estimated from the soft x-ray measurements assuming negligible radial variation of Z_{eff} and n_e. The PEST/VACUUM code permits the inclusion of a perfectly conducting wall with one poloidal gap. In order to simulate the two poloidal gaps present when the shells are retracted, the model shell is extended away from the plasma near the outer midplane as shown in Fig. 4(a).

Several points from the diagram bear notice. First, the stability limit to $n=1$ external kinks with the shells retracted is very similar to that obtained with the conducting shells at infinity. This indicates that completely retracting the shells produces a good approximation to a configuration with no conducting wall in HBT-EP. Second, with the segmented conducting shell inserted, the attainable value of normalized beta is predicted to double at $q(a)=2.8$. Finally, ballooning modes may also appear in kink-stabilized discharges, although the degree to which they may degrade the plasma is not known. The discharges associated with the experimental data points shown in the figure are discussed in detail below.

The role of β_N in the stability of rapidly formed discharges may be seen in Fig. 5. Here we compare two $q^*<3$ plasmas with β_N values of 0.8 and 1.3, respectively. In both cases, the shells are fully retracted. The time evolution of the normalized beta, which can be expressed as $\beta_N(t)=20\epsilon(t)\beta_p(t)/q^*(t)$, is estimated using magnetic measurements of the poloidal beta from toroidal force balance.[20] This involves combining the vertical field due to currents in the poloidal field coils, the conducting shells, and the vacuum chamber. The internal inductance was estimated using internal magnetic probe measurements from lower-

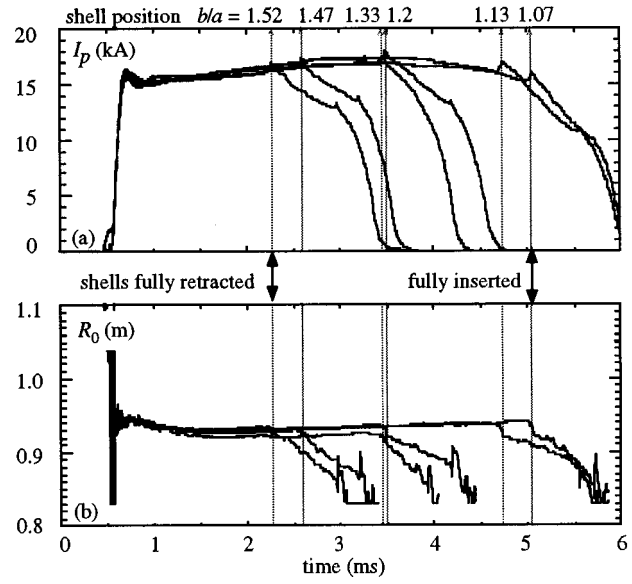

FIG. 6. (a) Evolution of the plasma current and (b) magnetic axis for similar discharges showing effect of conducting shell position, b, with respect to the surface of the plasma, a. Suppression of β-limiting disruptions occurs for $dI_p/dt>0$ and $b/a<1.2$.

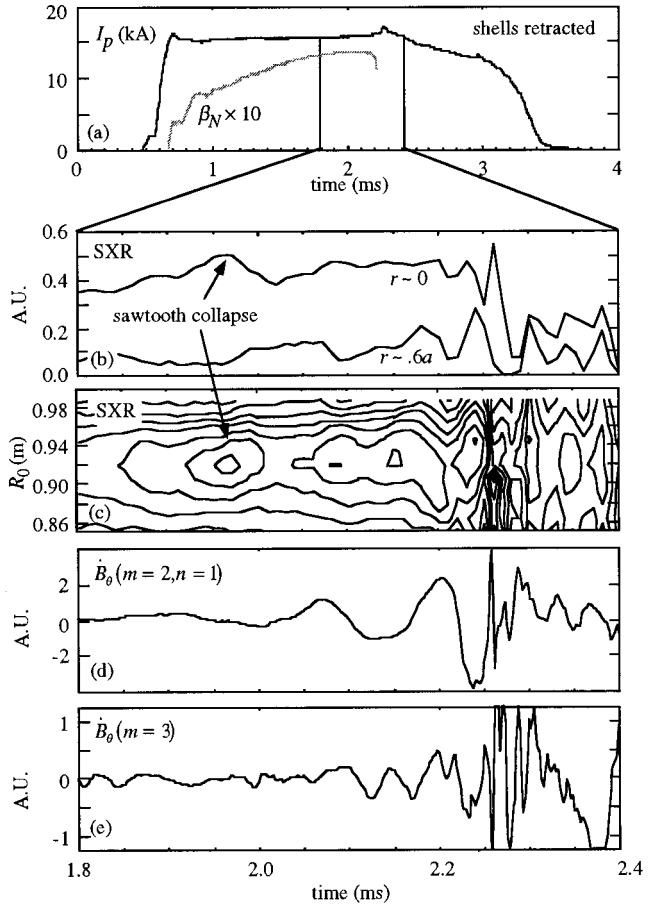

FIG. 7. Disruption sequence for discharge formed with the conducting shells fully retracted ($b/a=1.52$). (b) Sawtooth-like collapse leads to growth of global instability showing (d) $m/n=2/1$, (e) 3/2 and finally 3/1 magnetic perturbations. (c) Soft x-ray contours show strong $m=1$ displacement prior to thermal collapse.

temperature discharges and transport simulations. The $q^*<3$, low-β_N discharge was produced by reducing both the plasma current and the minor radius. The stability properties of the two discharges are quite distinct: the higher-β_N plasma disrupts at $\beta_N \sim 1.3$ with large-scale precursor oscillations while the lower-β_N shot remains quiescent.

In Fig. 6, the evolution of the plasma current and radial position are compared for six similar discharges in which position of the conducting shells was systematically varied with respect to the plasma surface. With the shells retracted, the plasma was terminated by a disruptive instability at $\beta_N \sim 1.3$. A clear relationship may be seen between the proximity of the conducting shells to the plasma and the plasma lifetime. Evident in this data, and supported by larger data sets is the indication that discharge-terminating disruptions are prevented if a moderate current ramp is maintained ($dI_p/dt \sim 0.5$ MA/s) and the shells are positioned such that $b/a<1.2$. Note that the plasmas formed with close-fitting shells eventually disrupt, although these disruptions occur during the current ramp-down phase and appear to be caused by slowly growing internal instabilities.

The termination mechanism for β-limited discharges can be elucidated by a closer examination of the disruption precursors. Figure 7 displays the sequence of events that lead to a disruption with the shells fully retracted ($b/a=1.52$). The termination sequence appears to have been initiated by changes within the plasma core, where a sawtooth-like collapse of the soft x-ray profile precipitated the growth of instabilities characterized by $m/n=2/1$ and 3/2 magnetic fluctuations. Approximately 20 μs prior to the complete collapse of the soft x-ray profile, magnetic field detectors indicated the growth of an $m=3$, $n=1$ perturbation with a large internal $m=1$ component as shown by soft x rays. A plasma current "spike" ($\delta I_p/I_p \approx 10\%$) appeared coincident with the thermal collapse, at which time radial equilibrium was lost.

Figure 8 shows the MHD activity in a similar discharge formed with the shells completely inserted ($b/a=1.07$). Although both $m=2$ and $m=3$ components were present, the growth rates and amplitudes of the fluctuations were reduced and the mode appeared to have no deleterious effects on the plasma as long as a moderately positive current ramp was maintained.

B. Residual instabilities in wall-stabilized discharges

Although the segmented conducting shells, when positioned sufficiently close to the surface of the plasma, prevented the growth of large-scale disruptive instabilities, Mirnov coils and soft x-ray measurements detected slowly growing and saturated rotating perturbations in these discharges. Instabilities with $m/n=1/1$, 2/1, and 3/1 components are routinely observed in "wall-stabilized" discharges (that is, discharges in which rapidly growing disruptive instabilities are suppressed by the conducting shells). The perturbations rotate in the electron drift direction and generally possess the same frequency. In addition, the m/n

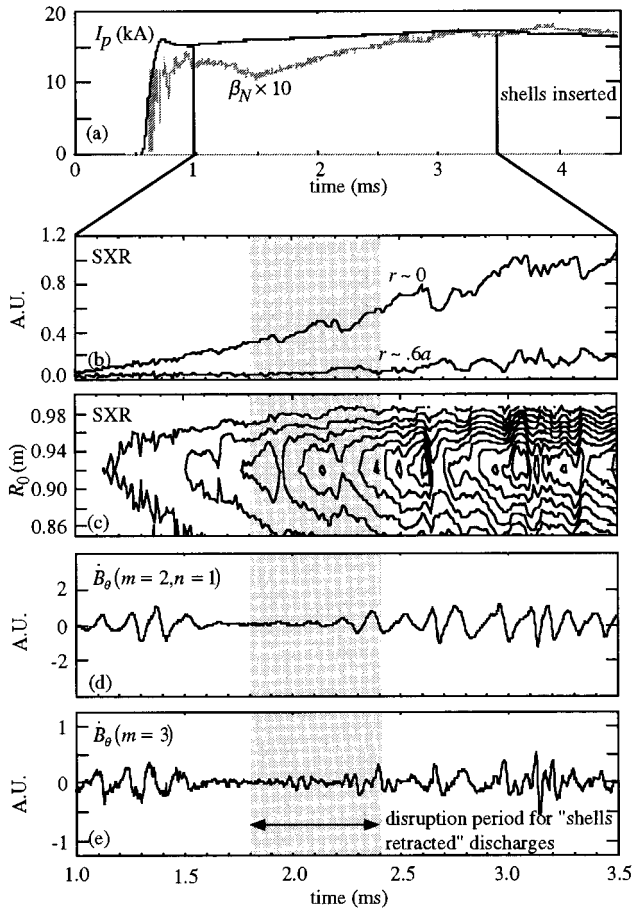

FIG. 8. (a) Plasma formed with the shells fully inserted ($b/a=1.07$) exceeds $\beta_N \sim 1.5$, limited by available Ohmic heating power. Internal fluctuations (b)–(e) do not lead to disruption during the current-ramp phase.

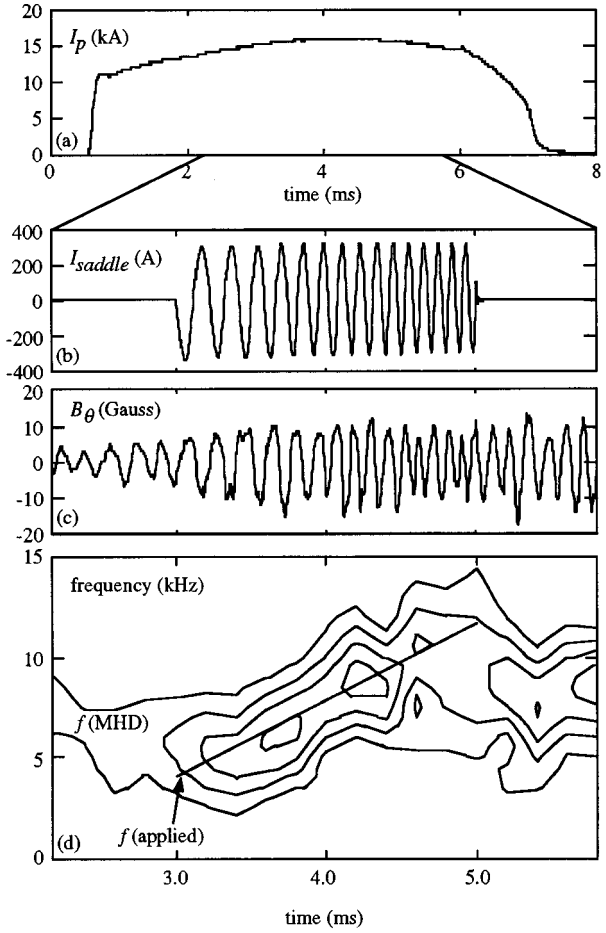

FIG. 9. Imposition of an oscillating, frequency-modulated $m=2$, $n=1$ resonant magnetic perturbation using the modular saddle coil array results in controlled acceleration of a slowly growing $m/n=2/1$ internal instability.

$=3/2$ perturbation is occasionally visible at twice the frequency of the $n=1$ components, implying rigid toroidal rotation. As previously noted, these instabilities often precede disruptions in the ramp-down ($dI_p/dt<0$) phase of the discharge even in the presence of the close-fitting shells. Indeed, internal, current-gradient-driven tearing modes, particularly the $m=2$, $n=1$, have long been associated with disruptions in tokamaks.[21] A means to control such instabilities in HBT-EP is presented in the following section.

C. Active control of MHD instabilities

The indication that disruptions with slowly growing precursors may occur in plasmas formed with the shells positioned close to the plasma points to the necessity of providing an active means of suppressing the growth of residual instabilities in wall-stabilized discharges. The approach taken in HBT-EP utilizes the application of oscillating magnetic perturbations for mode rotation control and closed-loop synchronous feedback for mode suppression. Both are accomplished using the high-power amplifiers with the modular saddle coil set described in Sec. II B.

1. Mode locking to rotating external magnetic perturbations

The HBT-EP saddle coils are positioned outside the vacuum chamber at the locations of the five quartz insulating gaps. This coincides with the spaces between the segmented conducting shells, and allows the applied field to be imposed upon the plasma with relatively little distortion by the shells. Previously-reported experiments[14] demonstrated that the magnetic field created by this compact coil set could produce a strong interaction with the plasma. Application of an $I_{sc} \approx 600$ A quasistatic pulse to the coils resulted in the slowing and locking of pre-existing $m=2$, $n=1$ fluctuations. This level of current corresponded to a toroidally averaged applied field at the resonant surface of $B_r(r_s) \approx 4$ G $\approx 1 \times 10^{-3} B_\phi$. Similar locking thresholds have been reported in tokamaks employing large-area saddle coils[22] and helical coils.[23] Greater levels of saddle coil current produced stimulated disruptions, as has been observed in earlier resonant magnetic perturbation experiments.[24,25]

Here, we report on the ability to influence the mode rotation velocity by imposing oscillating resonant magnetic perturbations on the plasma. Figure 9 displays a plasma formed with the shells completely inserted which exhibited

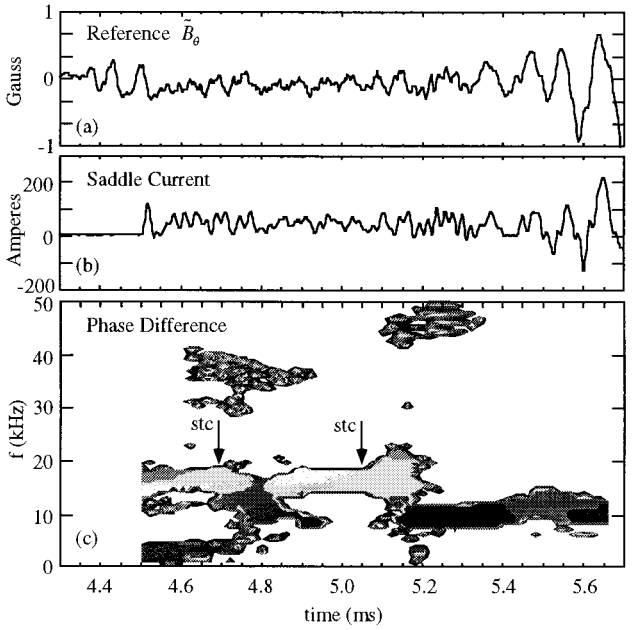

FIG. 10. Synchronous feedback using a time-delay circuit between (a) the reference signal and (b) the saddle coil drive. (c) Time evolution of the dominant frequency components of (a); mode growth follows change of frequency and phase difference (shaded contours) between (a) and (b). Arrows indicate sawtooth collapse events.

$m/n=2/1$ fluctuations of nearly constant amplitude. At $t=3$ ms, an $I_{0sc}\approx 350$ A oscillating current was applied to the saddle coils. The frequency of the applied field was ramped linearly from 4 kHz to 12 kHz over a period of 2 ms. The pre-existing plasma fluctuations decelerated, locked to the applied perturbation, and accelerated with the applied field over the frequency range $f_{\mathrm{MHD}}=5$–12 kHz. After the applied perturbation was removed, the plasma mode relaxed to the natural rotation frequency of $f_{\mathrm{MHD}}\approx 8$ kHz in a time $\tau_M\approx 500$ μs. Controlled deceleration of instabilities was carried out over the same frequency range in similar discharges.

2. Synchronous magnetic feedback

Synchronous magnetic feedback, a method whereby the phase and amplitude of the instability are detected and an opposing magnetic perturbation is applied, has shown promise as a technique for controlling internal instabilities in tokamaks.[26,27] Closed-loop feedback experiments have been initiated on HBT-EP by using a time-delay control scheme. For this experiment, a pickup coil mounted on the plasma-facing side of a conducting shell was used to sense magnetic fluctuations due to a plasma instability. The signal was partially integrated, time delayed, and input to the saddle coil power amplifiers. Figure 10 displays the time evolution of the reference signal, saddle coil current, and phase difference between the signals as a function of frequency for a case in which the time delay was adjusted to be 50 μs. The saddle coils were energized at $t=4.5$ ms, at which time a significant reduction in the $f=15$ kHz mode amplitude was observed. A change in mode frequency of $\Delta f\approx 5$ kHz occurred at $t\approx 5.1$ ms following a sawtooth collapse and resulted in a $\sim 90°$ change in the relative phase of the input and output signals, as expected for a feedback scheme based on a simple time delay between signals. The mode growth following the change in frequency is attributed to an unfavorable phase relationship between the detected signal and the feedback response. Although the data indicate that time-delay feedback can reduce the amplitude of modes present in wall-stabilized discharges, the example exposes the inability of a time-delay system to maintain negative feedback as the mode frequency changes. A more sophisticated arrangement employing a phase-locked loop is presently being tested.

IV. DISCUSSION AND SUMMARY

The segmented shells have been shown to suppress the growth of β-limiting instabilities in HBT-EP discharges. The disruptions caused by these instabilities when the shells were retracted were initiated in the core of the plasma as indicated by a sawtooth-like collapse of the soft x-ray profile. The presumed broadening of the current profile caused by this event gave rise to the rapidly growing global mode (displaying $m=1$, 2, and 3 components) that terminated the discharge. Although soft x-ray collapses of this nature were routinely observed in plasmas formed with the shell inserted, the resultant growth of the $m=2$ and $m=3$ components was mitigated and disruptions were eliminated. Preliminary experiments indicate that plasmas formed with only 50% of the shells fully inserted also undergo significant wall stabilization, possibly a result of the natural rotation of the plasmas in HBT-EP.

To date, HBT-EP has relied solely on Ohmic power for plasma heating. This has restricted the maximum β_N to ~ 2 (limited by transport) for plasmas of $\langle T_e\rangle \geqslant 50$ eV. The planned addition of 100 kW of ICRF heating will allow HBT-EP to probe the boundary above which kink modes are again predicted to become unstable with the segmented shells fully inserted [see Fig. 4(c)].

The resistive wall mode has not been unambiguously identified in HBT-EP, although the predicted slow growth of the instability combined with the presence of other slowly growing internal modes may obscure its diagnostic signature. There is, however, theoretical[28] evidence that rapid rotation combined with plasma dissipation can stabilize this mode. Typically, the natural rotation frequency of HBT-EP plasmas inferred from Mirnov oscillations is found to be $f_{\mathrm{MHD}}>6$ kHz ($v_\phi>35$ km/s$=0.6v_S=0.02v_{\mathrm{A}}$, where v_S is the ion sound speed and where v_{A} is the toroidal Alfvén velocity). Experimental data from the DIII-D tokamak[29] suggests that this level of rotation may be sufficient to stabilize the resistive wall mode.

The ability to provide rotation control using a series-connected (single-phase) saddle coil set may be heuristically understood by considering that an oscillating current applied to the coil set generates, in effect, electromagnetic waves traveling in opposite toroidal directions. Theoretically,[30] the torque exchanged between the applied perturbations and the rotating plasma occurs near the resonant surface [in this case $q(r_s)=2/1$], and the strength of this interaction is a nonlinear function of the frequency difference between the applied perturbation and the rotating magnetic island that generates the measured fluctuations. The plasma will seek to maintain a

natural mode rotation velocity through a viscous restoring torque—a linear function of the mismatch between the mode rotation velocity and the plasma rotation velocity. For the single-phase saddle coils, the large frequency difference between the rotating island and applied perturbation traveling opposite the island results in a negligible electromagnetic torque which is easily overcome by the viscous drag of the plasma (the so-called ''high-slip'' condition). Thus, only the component of the applied perturbation traveling with the mode provides substantial coupling to the plasma. The advantage of a single-phase system is simplicity, albeit at the expense of increased power requirements over a multiphased array of saddle coils.

In summary, results from the conducting shell experiments demonstrate that fast-growing, low-n kink instabilities were suppressed if the shells were positioned sufficiently near the surface of the plasma ($b/a<1.2$) and a positive dI_p/dt was maintained. Wall stabilization was observed both in plasmas with strong current ramps and in discharges near the Troyon limit. Active control of internal instabilities in shell-stabilized plasmas was demonstrated using frequency-modulated resonant magnetic perturbations applied by a compact set of $m=2$, $n=1$ saddle coils. In addition to providing plasma rotation control, this method may be extended by using an additional saddle coil set to induce differential rotation of multiple resonant surfaces within the plasma. The resulting shear in the plasma flow velocity is predicted to produce enhanced stability and confinement.[31]

ACKNOWLEDGMENTS

It is a pleasure to acknowledge the HBT-EP technical staff, M. Cea, N. Rivera, and E. Rodas for their dedication in maintaining the steady operation of the tokamak, H. Alvestad for his effort in installing the Los Alamos National Laboratory power amplifiers, J. Manickam and M. Chance for their invaluable assistance with the PEST and VACUUM codes, and D. Gates for useful discussions.

This work is supported by the U.S. Department of Energy under Grant No. DE-FG02-86ER-53222.

[1]F. Najmabadi and R. W. Conn, in *Plasma Physics and Controlled Nuclear Fusion Research*, Würzburg, 1992 (International Atomic Energy Agency, Vienna, 1993), Vol. 3, p. 295.
[2]R. Fitzpatrick, Phys. Plasmas **1**, 2931 (1994).
[3]J. P. Goedbloed, D. Pfirsch, and H. Tasso, Nucl. Fusion **12**, 649 (1972).
[4]E. J. Strait, Phys. Plasmas **1**, 1415 (1994).
[5]F. Troyon, R. Gruber, H. Saurenmann, S. Semenzato, and S. Succi, Plasma Phys. Controlled Fusion **26**, 209 (1984).
[6]J. L. Luxon, R. Anderson, F. Batty, C. B. Baxi, G. Bramson, N. H. Brooks, B. Brown, B. Burley, K. H. Burrell, R. Callis, G. Campbell, T. N. Carlstrom, A. P. Colleraine, J. Cummings, L. Davis, J. C. DeBoo, S. Ejima, R. Evanko, H. Fukomoto, R. Gallix, J. Gilleland, T. Glad, P. Gohil, A. Gootgeld, R. J. Groebner, S. Hanai, J. Haskovec, E. Heckman, M. Heilberger, F. J. Helton, N. Hosogane, C.-L. Hsieh, G. L. Jackson, G. Jahns, G. Janeschitz, E. Johnson, A. G. Kellman, J. S. Kim, J. Kohli, A. Langhorn, L. L. Lao, P. Leek, S. Lightner, J. Lohr, M. A. Mahdavi, M. Mayberry, B. McHarg, T. McKelvey, R. Miller, C. P. Moeller, D. Moore, A. Nerem, P. Noll, T. Ohkawa, N. Ohyabu, T. H. Osborne, D. O. Overskei, P. I. Petersen, T. W. Petrie, J. Phillips, R. Prater, J. Rawls, E. E. Reis, D. Remsen, P. Riedy, P. Rock, K. Schaubel, D. P. Schissel, J. T. Scoville, R. Seraydarian, M. Shimada, T. Shoji, B. Sleaford, J. P. Smith, Jr., T. Smith, R. T. Snider, R. D. Stambaugh, R. Stav, H. St. John, R. E. Stockdale, E. J. Strait, R. Stree, T. S. Taylor, J. Tooker, M. Tupper, S. K. Wong, and S. Yamaguchi, in *Plasma Physics and Controlled Nuclear Fusion Research*, Kyoto, 1986 (International Atomic Energy Agency, Vienna, 1987), Vol. 1, p. 159.
[7]E. J. Strait, T. S. Taylor, A. D. Turnbull, J. R. Ferron, L. L. Lao, B. Rice, O. Sauter, S. J. Thompson, and D. Wróblewski, Phys. Rev. Lett. **74**, 2483 (1995).
[8]M. Okabayashi, K. Bol, M. Chance, P. Couture, H. Fishman, R. J. Fonck, G. Gammel, W. W. Heidbrink, K. Ida, K. P. Jaehnig, G. Jahns, R. Kaita, S. M. Kaye, H. Kugel, B. LeBlanc, J. Manickam, W. Morris, G. A. Navratil, N. Ohyabu, S. Paul, E. Powell, M. Reusch, S. Sesnic, and H. Takahashi, in *Plasma Physics and Controlled Nuclear Fusion Research*, Kyoto, 1986 (International Atomic Energy Agency, Vienna, 1987), Vol. 1, p. 275.
[9]R. Bell, N. Asakura, S. Bernabei, M. S. Chance, P.-A. Duperrex, R. J. Fonck, G. M. Gammel, G. Greene, R. E. Hatcher, A. Holland, S. C. Jardin, T.-W. Jiang, R. Kaita, S. M. Kaye, C. E. Kessel, H. W. Kugel, B. LeBlanc, F. M. Levinton, M. Okabayashi, M. Ono, S. F. Paul, E. T. Powell, Y. Qin, D. W. Roberts, N. R. Sauthoff, S. Sesnic, and H. Takahashi, Phys. Fluids B **2**, 1271 (1990).
[10]T. C. Hender, C. G. Gimblett, and D. C. Robinson, Nucl. Fusion **29**, 1279 (1989).
[11]M. F. F. Nave and J. A. Wesson, Nucl. Fusion **30**, 2575 (1990).
[12]J. A. Snipes, D. J. Campbell, P. S. Haynes, T. C. Hender, M. Hugon, P. J. Lomas, N. J. Lopes Cardozo, M. F. F. Nave, and F. C. Schüller, Nucl. Fusion **28**, 1085 (1988)
[13]M. K. V. Sankar, E. Eisner, A. Garofalo, D. Gates, T. H. Ivers, R. Kombargi, M. E. Mauel, D. Maurer, D. Nadle, G. A. Navratil, and Q. Xiao, J. Fusion Energy **12**, 303 (1993).
[14]T. H. Ivers, E. Eisner, A. Garofalo, D. Gates, R. Kombargi, M. E. Mauel, D. Maurer, D. Nadle, G. A. Navratil, M. K. V. Sankar, and Q. Xiao, ''Passive and Active Control of MHD Instabilities in the HBT-EP Tokamak,'' *Plasma Physics and Controlled Nuclear Fusion Research*, Seville, 1994 (International Atomic Energy Agency, Vienna, in press).
[15]W. A. Reass, J. G. Garcia, R. J. Kasik, and A. M. Velasquez, in *Proceedings of the 12th Symposium on Fusion Engineering*, Monterey (Institute of Electronics and Electrical Engineers, New York, 1987), p. 385.
[16]J. A. Wesson, Nucl. Fusion **18**, 87 (1978).
[17]G. Eriksson and C. Wahlberg, Phys. Rev. Lett. **72**, 2713 (1994).
[18]M. S. Chance, R. L. Dewar, A. M. M. Todd, J. Manickam, R. C. Grimm, J. M. Greene, and J. L. Johnson, in *Proceedings of the Eighth Conference on Numerical Simulation of Plasmas*, Monterey, CA, Division of Magnetic Fusion Energy, Division of Laser Fusion (U.S. Department of Energy, Washington, DC, 1978).
[19]J. Manickam, R. C. Grimm, and R. L. Dewar, Comp. Phys. Comm. **24**, 355 (1981).
[20]T. H. Ivers, D. Gates, T. C. Marshall, M. E. Mauel, G. A. Navratil, V. Sankar, and J. Wang, in *Plasma Physics and Controlled Nuclear Fusion Research*, Washington, DC, 1990 (International Atomic Energy Agency, Vienna, 1991), Vol. 1, p. 573.
[21]J. C. Hosea, C. Bobeldijk, D. J. Grove, in *Plasma Physics and Controlled Nuclear Fusion Research*, Madison, 1970 (International Atomic Energy Agency, Vienna, 1971), Vol. II, p. 425.
[22]K. Bol, J. L. Cecci, C. C. Daughney, F. DeMarco, R. A. Ellis, Jr., H. P. Eubank, H. P. Furth, H. Hsuan, E. Mazzucato, and R. R. Smith, in *Plasma Physics and Controlled Nuclear Fusion Research*, Tokyo, 1974 (International Atomic Energy Agency, Vienna, 1975), Vol. 1, p. 83.
[23]D. E. Roberts, D. Sherwell, J. D. Fletcher, G. Nothnagel, and J. A. M. de Villiers, Nucl. Fusion **31**, 319 (1991).
[24]F. Karger, H. Wobig, S. Corti, J. Gernhardt, O. Klüber, G. Lisitano, K. McCormick, D. Meisel, and S. Sesnic, in *Plasma Physics and Controlled Nuclear Fusion Research*, Tokyo, 1974 (International Atomic Energy Agency, Vienna, 1975), Vol. 1, p. 207.
[25]T. C. Hender, R. Fitzpatrick, A. W. Morris, P. G. Carolan, R. D. Durst, T. Edlington, J. Ferreira, S. J. Fielding, P. S. Haynes, J. Hugill, I. J. Jenkins, R. J. La Haye, B. J. Parham, D. C. Robinson, T. N. Todd, M. Valovic, and G. Vayakis, Nucl. Fusion **32**, 2091 (1994).
[26]V. V. Arsenin, L. I. Artemenkov, N. V. Ivanov, A. M. Kakurin, L. I. Molotkov, A. N. Chudnovskij, N. N. Shvindt, Yu. V. Gvozdkov, and M. Yu. Cherkashin, in *Plasma Physics and Controlled Nuclear Fusion Research*, Innsbruck, 1978 (International Atomic Energy Agency, Vienna, 1975), Vol. 1, p. 233.
[27]A. W. Morris, T. C. Hender, J. Hugill, P. S. Haynes, P. C. Johnson, B.

Lloyd, D. C. Robinson, C. Silvester, S. Arshad, and G. M. Fishpool, Phys. Rev. Lett. **64**, 1254 (1990).
[28]A. Bondeson and D. J. Ward, Phys. Rev. Lett. **72**, 2709 (1994).
[29]T. S. Taylor, E. J. Strait, L. L. Lao, M. Mauel, A. D. Turnbull, K. H. Burrell, M. S. Chu, J. R. Ferron, R. J. Groebner, R. J. La Haye, B. W. Rice, R. T. Snider, S. J. Thomson, D. Wròblewski, and D. J. Lightly, Phys. Plasmas **2**, 2390 (1995).
[30]T. H. Jensen, A. W. Leonard, and A. W. Hyatt, Phys. Fluids B **5**, 1239 (1993).
[31]T. H. Jensen and A. W. Leonard, Phys. Fluids B **3**, 3422 (1991).